LAWRENCE
LIVERMORE
NATIONAL
LABORATORY

LLNL-JRNL-411318

# Vapor-liquid phase equilibria of water modelled by a Kim-Gordon potential

K. A. Maerzke, M. J. McGrath, I.-F. W. Kuo, G. Tabacchi, J. I. Siepmann, C. J. Mundy

March 17, 2009

Chemical Physics Letters

## Disclaimer

# Vapor–liquid phase equilibria of water modelled by a Kim-Gordon potential

Katie A. Maerzke[a], Matthew J. McGrath[a,1], I.-F. William Kuo[b], Gloria Tabacchi[c], J. Ilja Siepmann[*,a], Christopher J. Mundy[**,d]

[a]*Departments of Chemistry and of Chemical Engineering and Materials Science, University of Minnesota, 207 Pleasant Street SE, Minneapolis, MN 55455*

[b]*Chemical Sciences Division, Lawrence Livermore National Laboratory, P. O. Box 808, Livermore, CA 94551*

[c]*Dipartimento di Scienze Chimiche de Ambientali (DSCA), Universita' dell'Insubria and INSTM, Via Lucini 3, 1-22100 Como, Italy*

[d]*Chemical & Materials Sciences Division, Pacific Northwest National Laboratory, Richland, WA 99352*

## Abstract

Gibbs ensemble Monte Carlo simulations were carried out to investigate the properties of a frozen-electron-density (or Kim-Gordon, KG) model of water along the vapor–liquid coexistence curve. Because of its theoretical basis, such a KG model provides for seamless coupling to Kohn-Sham density functional theory for use in mixed quantum mechanics/molecular mechanics (QM/MM) implementations. The Gibbs ensemble simulations indicate rather limited transferability of such a simple KG model to other state points. Specif cally, a KG model that was parameterized by Barker and Sprik to the properties of liquid water at 300 K, yields saturated vapor pressures and a critical temperature that are signif cantly under- and overestimated, respectively.

## 1. Introduction

Water is an interesting and important system to study due to its unique properties, its importance in biological and environmental systems, and because it is the prototypical example of hydrogen-bond former. Liquid water was one of the f rst molecular systems studied by particle-based simulation methods [1, 2]. However, water's large dipole moment, the importance of many-body polarization effects for its condensed phases, and the directional nature of the hydrogen bond pose a challenge for development of accurate and eff cient water models. Hence, models with different complexity have been used for simulations of water and aqueous systems ranging from relatively simple, but eff cient non-polarizable models [3, 4] over more sophisticated polarizable models [5, 6, 7] to f rst principles representations based on Kohn-Sham density functional theory (KS-DFT) [8, 9, 10, 11]. Given the dramatic increase in computational expense with increasing complexity of the model, it is often preferable to use a multi-scale method that describes different regions of the physical system with different models. QM/MM (quantum mechanics/molecular mechanics) approaches, where a small region of interest is treated using an electronic structure method and the remainder of the system is treated with molecular mechanics models, have proven

[*]Corresponding author. Email: siepmann@umn.edu

[**]Corresponding author. Email: chris.mundy@pnl.gov

[1]Present address: Department of Chemistry, University of Dschang, B.P. 67, Cameroon, West Africa

particularly powerful [12, 13, 14]. Frozen-electron-density or Kim-Gordon (KG) models [15, 16] have been considered as a potential intermediate between explicitly optimized electronic structure representations and molecular mechanics, as they would allow for a more seamless transitions between the QM and MM regions.

Recently, Barker and Sprik (BS) developed a KG model for water [17] which accurately reproduces the liquid structure at 300 K and a fixed density of 0.997 g/mL. The fully empirical Enhanced Dipole Pseudo Density (EDPD5) KG model (called BS-KG model throughout this manuscript) was parameterized to have a dipole moment of 2.95 D, in agreement with the data obtained from Car-Parrinello molecular dynamics simulations for liquid water represented by the BLYP density functional [9, 18, 19]. In addition, the OH bond length of $r_{\mathrm{OH}} = 0.991$ Å and HOH angle of 105.5° were chosen in order to reproduce the average condensed phase molecular geometry of the same first principles simulation [9]. Barker and Sprik found good agreement for structural and dynamic properties of a KG model with judiciously chosen parameters (EDPD5) and experiment [17]. It is a remarkable success that a semi-empirical model (with $\mathcal{O}(N)$ scaling) based in pure DFT using the BLYP exchange-correlation functionals is able to yield a satisfactory water structure. In contrast, KS-DFT in conjunction with BLYP leads to an over-structured liquid (at fixed density). Moreover, the KG formulation also allows one to isolate the effects of the basis set and the kinetic energy operator within the KS-DFT formulation while keeping the exchange-correlation functional fixed to better understand the dominant contributions to the over-structuring of liquid water using BLYP in conjunction with KS-DFT.

In order to assess the transferability of the BS-KG model to different thermodynamic states, we used Gibbs ensemble Monte Carlo simulations [20, 21, 22] to determine its vapor–liquid coexistence curves and to investigate the structure of the saturated liquid phase. One should keep in mind that the BS-KG model contains an electronic density parameterized to liquid water at a specific state point and this frozen density cannot adapt to the environment (as is also the case for non-polarizable water models). As will be shown, the BS-KG model is not transferable to other state points and, likely, can also not be applied to mixtures or heterogeneous systems, e.g. water near solid substrates or non-polar regions of a protein.

## 2. Simulation Details

Gibbs ensemble Monte Carlo [20, 21] simulations were carried out in the canonical ($NVT$) ensemble in order to compute the vapor–liquid coexistence densites, saturated vapor pressures, and heats of vaporization for the BS-KG model. These simulations follow a protocol similar to one employed previously by this group for the determination of the vapor–liquid coexistence curves for water modelled by various density functionals [22, 23]. The energy calculations for the BS-KG model were performed using the efficient Quickstep [24] and KG [25] routines of the publically available CP2K package (http://cp2k.berlios.de). The Gibbs ensemble simulations [20] utilizes two separate periodic simulation boxes in thermodynamic contact, but without an explicit interface. Since the internal structure of water is kept rigid in the BS-KG model, the Gibbs ensemble simulations employ four different types of moves (translations, rotations around the center of mass, and volume and particle exchanges between the two simulation boxes). In order to increase the efficiency of the simulations, pre-biasing with an inexpensive potential was used for translations and rotations [10, 26, 27], and configurational-bias strategies [22, 28, 29, 30, 31] were used for particle swap moves.

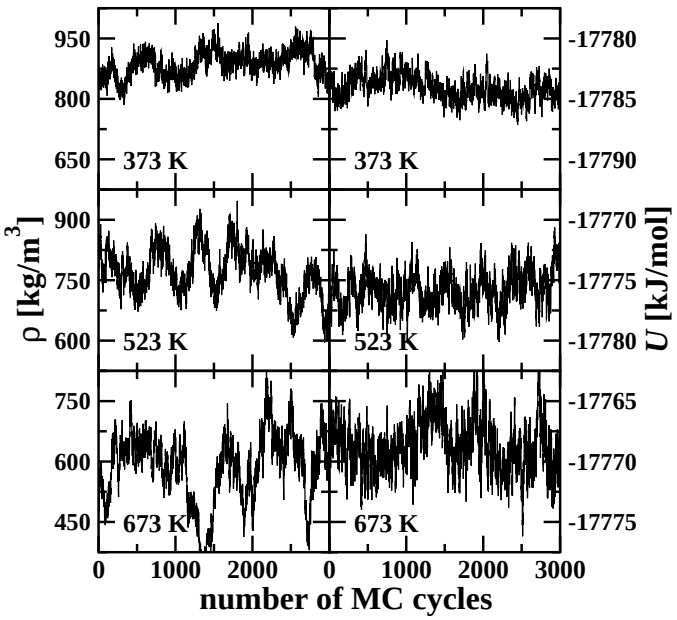


**Figure 1:** Instantaneous liquid-phase densities and energies at $T$ =373 K, 523 K, and 673 K as a function of MC cycle.

All Gibbs ensemble simulations for the BS-KG model were carried out for a system containing a total of 64 molecules and with the volumes of the vapor- and liquid-phase boxes being approximately equal, which previous simulations have shown to be a set-up suff cient to avoid signif cant f nite-size effects [22]. In the empirical BS-KG water model, the electron density is modelled by using only one atom-centered Gaussian function per nucleus. Specif cally, the electron density def ning parameters (i.e. Gaussian exponent and coeff cients) are $\alpha_H = 0.568$; $q_H = -0.200$ for hydrogen and $\alpha_O = 0.53$; $q_O = -5.022$ for oxygen. The kinetic and exchange correlation energy terms were treated with the gradient-corrected kinetic energy functional LLP [32]. A plane-wave cutoff of 600 Ry was used for the electronic density in all simulations as this cutoff was shown to be necessary to prevent artifacts in moves that change the volume of a simulation box (and consequently the number of grid points used for the energy evaluation) [33].

Simulations at 373, 473, and 573 K were initialized using conf gurations from previous simulations for the BLYP representation, but with the molecular conformations adjusted to those for the rigid BS-KG model. The f nal structures from these simulations were then used to spawn simulations at other temperatures, and the vapor–liquid coexistence curve is well represented by 8 simulations covering the temperature range from 373 to 673 K. The simulations were equilibrated for at least 1000 Monte Carlo cycles (where one cycle consists of 64 randomly selected moves), and 3000 cycles were employed for the standard production period. The exception was the run at 573 K that was continued for a total production period of 9000 cycles, but no signif cant differences were observed between the shorter and longer production periods. Here it should be noted that the number of accepted particle phase-transfer moves at 373 K was too low to allow for a determination of the coexistence properties, and only the liquid-phase properties (at near-zero pressure) can be estimated from this simulation.

To estimate the statistical uncertainties of the simulations, the standard error of the mean was calculated by dividing the production periods into 3 blocks. Figure 1 shows the evolution of the

instantaneous density and potential energy of the liquid phase at three temperatures; no signif cant drift is observed in any of these properties over the length of the production period. As an aside, we note here that the molar energies of the liquid phase for the BS-KG model differ signif cantly from those found for saturated liquid phases described by the BLYP representation [22]. The pseudo-density of the empirical KG-BS model is constructed in such a way to model only the tail (i.e., the valence region) of the electronic distribution. Thus, the pseudo-density has been readjusted by a trial-and-error procedure in order to optimize it to the condensed phase environment, with the only constraint that the Gaussian parameters yield a value of 2.95 D for the dipole moment. With such an entirely empirical parametrization procedure, all information on absolute energies is lost, and only relative energies can be compared.

The critical temperature ($T_{\text{crit}}$) and density ($\rho_{\text{crit}}$) were estimated using the scaling law [34] for the simulation data at the f ve highest temperatures

$$\rho_{\text{liq}}(T) - \rho_{\text{vap}}(T) = B\,(T - T_{\text{crit}})^{\beta} \tag{1}$$

where $\beta = 0.325$ and the law of rectilinear diameters [35]

$$\tfrac{1}{2}\,(\rho_{\text{liq}}(T) + \rho_{\text{vap}}(T)) = \rho_{\text{crit}} + A\,(T - T_{\text{crit}}) \tag{2}$$

where $\rho_{\text{liq}}$ and $\rho_{\text{vap}}$ are the liquid and vapor densities, respectively. The normal boiling point ($T_{\text{boil}}$) was calculated using the Clausius-Clapeyron equation [36]

$$\frac{\mathrm{d}\ln P_{\text{vap}}}{\mathrm{d}T} = \frac{\Delta H_{\text{vap}}}{RT^2} \tag{3}$$

for the three temperatures nearest to $T_{\text{boil}}$.

We compare the results obtained here for the BS-KG model with previous Gibbs ensemble simulations for 64-molecule systems described by the BLYP functional with a triple-$\zeta$ basis set with two sets of $p$-type or $d$-type polarization functions (TZV2P) [22, 23]. These simulations for the BLYP functional were run for 350-450 Monte Carlo cycles, where the last 200 cycles were used for analysis. As these simulations were too expensive to perform multiple independent simulations and the runs were too short to divide into blocks, the error bars were estimated from the full width at half the maximum of the distribution. In contrast, the Gibbs ensemble simulations for the BS-KG model are signif cantly less expensive, which enabled us to carry out BS-KG simulations of suff cient length to allow for the determination of the statistical uncertainties from block averages.

## 3. Results and Discussion

A comparison of the vapor–liquid coexistence curves (VLCCs) for BS-KG and BLYP-TZV2P water is shown in Figure 2. The BS-KG model yields a VLCC that differs signif cantly from that for the BLYP-TZV2P representation and the deviations increase with increasing temperature. This ref ects that the dipole moment of the BS-KG model remains constant, whereas the average liquid-phase dipole moment for the BLYP-TZV2P representation decreases with increasing temperature [22, 37]. Extrapolating the saturated liquid densities to lower temperature yields rather similar densities for both models at 300 K, the temperature used in the parameterization of the BS-KG model. This may point to the def ciency that popular exchange-correlation functionals are lacking the correct asymptotic behavior for long range interactions, which could adversely effect

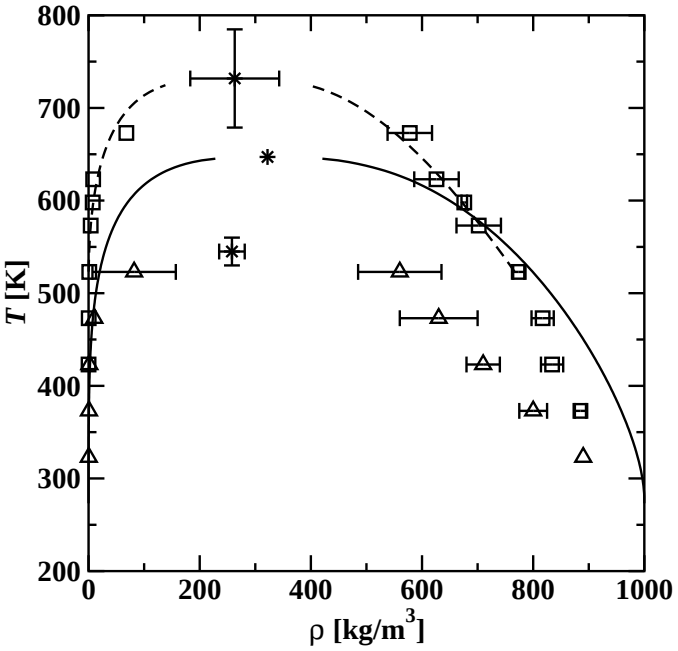


**Figure 2:** Vapor–liquid coexistence curves for BS-KG water (squares), BLYP-TZV2P water (triangles) [22, 23], and experiment (solid lines) [39]. The dashed lines indicate the scaling law f t for the BS-KG model. Error bars are explained in the text.

thermodynamic properties [38]. Already at 373 K, the saturated liquid density for the BS-KG model is about 10% higher than that for the BLYP-TZV2P representation. At 573 K, the saturated liquid density for the BS-KG model yields a fortuitous agreement with the experimental value. The saturated vapor densities for the BS-KG model are too low at all temperatures.

The BS-KG model severely overestimates the critical temperature, with a value of $T_{\text{crit}} = 732 \pm 53$ K compared to the experimental value of 647 K. Conversely, BLYP-TZV2P understimates the critical temperature, yielding a value of about 545 K [22]. The higher $T_{\text{crit}}$ for the BS-KG is likely an artifact of its f xed dipole moment. Nevertheless, both models yield a similar critical density of about 260 kg/m$^3$ (20% below the experimental value).

The vapor-phase pressures were not explicitly evaluated in these Gibbs ensemble simulations (because the calculation of the pressure via the virial route is far from trivial) and the saturated vapor pressures for the BS-KG model were estimated from the vapor densities using the same procedure as done previously for the BLYP-TZV2P data [22]. The results are shown in the Clausius-Clapeyron plot in Figure 3. The BS-KG model signif cantly underestimates the vapor pressures, especially at low temperatures. Using the Clausius-Clapeyron plot, we esimate a boiling point of $486 \pm 6$ K for the KG model. In this case, BLYP-TZV2P does reasonably well, with a boiling point of about 350 K [22].

The heats of vaporization are compared in Figure 4. As should be expected from the underestimation of the saturated vapor pressures, the BS-KG model overestimates the heat of vaporization by about 20 kJ/mol over the temperature range from 400-600 K, whereas the BLYP-TZVP representation yields much better agreement with experiment particular for intermediate temperatures. Even when extrapolating to 300 K, the BS-KG model clearly would yield a heat of vaporization

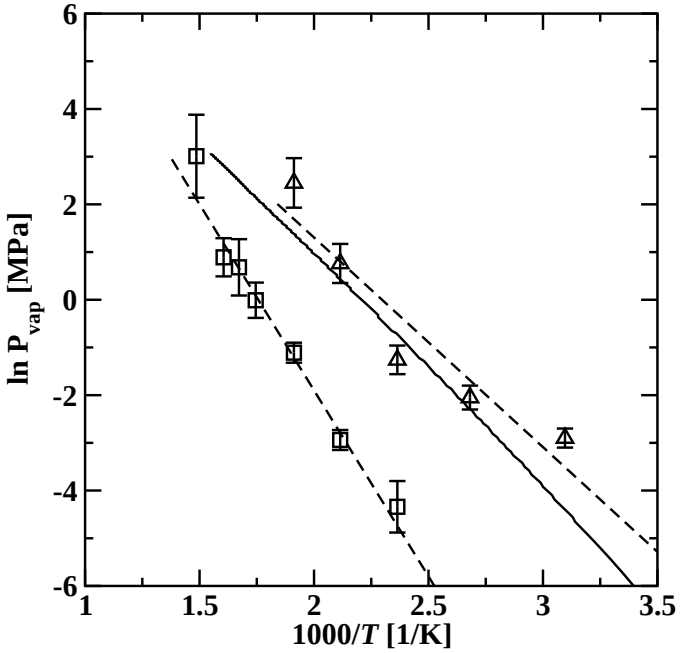


**Figure 3:** Clausius-Clapeyron plots showing the estimated vapor pressures for BS-KG (squares) and BLYP-TZV2P models (triangles) [23, 22], and the experimental data (solid lines) [39]. The dashed lines indicate a weighted linear f t for BS-KG and an unweighted linear f t for BLYP-TZV2P. Error bars are explained in the text.

much larger than BLYP-TZV2P despite that the former model is parameterized at this temperature. The reason for this shortcomings is the frozen-electron-density approximation, i.e., the electronic structure of a molecule being transferred from the liquid phase to the vapor phase cannot relax in the new environment and reach its gas-phase dipole moment of about 1.85 (or slightly higher average gas-phase dipole moments at elevated temperatures [22, 37]. Persisting in the gas phase with the larger f xed dipole moment appropriate for the liquid phase prevents the water molecule from recovering the energetic cost for polarization and, hence, the heat of vaporization is too large (and, correspondingly, the saturated vapor pressure too low). A similar problem has been previously noticed for non-polarizable water models, such as SPC/E, that include the polarization cost in the parameterization [4, 40, 41].

Figure 5 shows a comparison of the liquid structures for the saturated liquid phase of BS-KG and BLYP-TZV2P at 423 K. It should be noted that the saturated liquid density at 423 K obtained for the BS-KG model is about 17% larger than that for BLYP-TZV2P and 10% smaller than the experimental value. Due to the density difference the f rst peak in the oxygen–oxygen radial distribution function (RDF) is shifted to a smaller separation for the BS-KG model compared to BLYP-TZV2P. The f rst peak height in the oxygen–oxygen RDF is also lower for BS-KG than for BLYP-TZV2P, and both peak position and height for BS-KG agree very well with the values obtained for the polarizable TIP4P-pol2 model [6] that reproduce the experimental structure for water below the normal boiling point extremely well [42]. However, this agreement is at least to some extent fortuitous because the saturated liquid density at 423 K for the TIP4P-pol2 model is close the experimental value, i.e., higher than for the BS-KG model. The differences in the

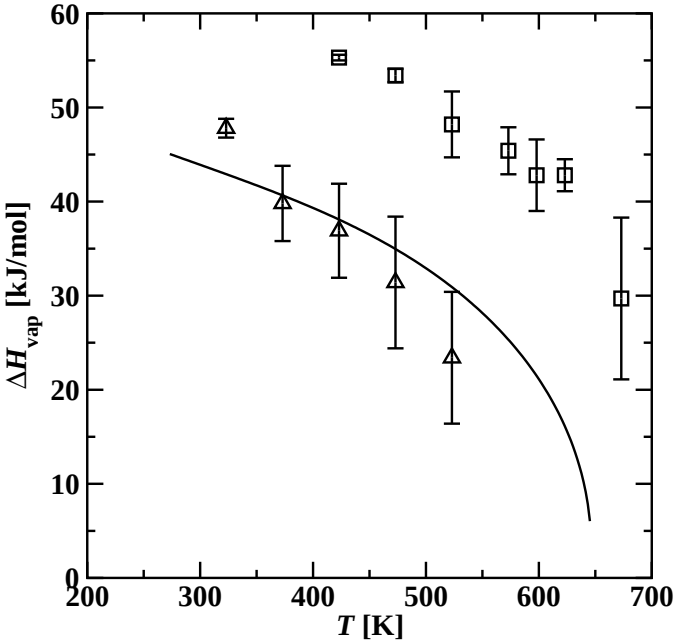


**Figure 4:** Heats of vaporization for BS-KG (squares), BLYP-TZV2P (triangles) [22, 22], and experiment (black lines) [39]. Error bars are explained in the text.

oxygen–hydrogen and hydrogen–hydrogen RDFs are less pronounced than for the oxygen–oxygen RDF, and neither the RDFs for the BS-KG nor the BLYP-TZV2P show a very good match of the first and second peaks and first minimum with the RDFs obtained for the TIP4P-pol2 model. Finally, it is worth noting that the BS-KG model yields RDFs with a significantly larger values at small separations.

## 4. Conclusions

Although frozen-electron-density models are computationally much more efficient than explicit KS-DFT representations, their transferability to other state points or other environments appears to be similarly limited as that for simple non-polarizable force fields. The frozen density approximation results in an overestimation of the heat of vaporization for the BS-KG model (and, presumably, also for the transfer free energy from a polar environment to an non-polar environment), an underestimation of the saturated vapor pressure, and an overestimation of the saturated liquid density at elevated temperatures. Although potentially useful for QM/MM simulations, additions of self-consistent polarization to the KG model would likely be needed for applications in chemical environments where the dipole moment of water is expected to differ from the value used in the parameterization. Nevertheless, there appears promise in the development of more efficient models that can seamlessly interface with KS-DFT representations.

## 5. Acknowledgements

KAM would like to acknowledge support from the Summer Research Institute at Pacific Northwest National Laboratory (PNNL). The work at the University of Minnesota is supported

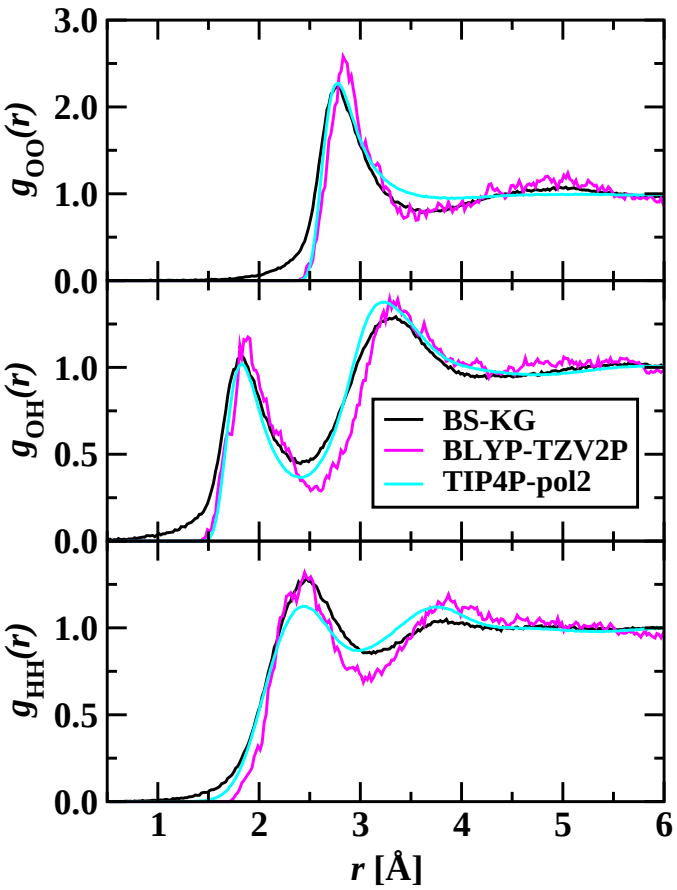


**Figure 5:** Intermolecular radial distribution functions for BS-KG (black), BLYP-TZV2P (cyan) [22, 23], and TIP4P-pol2 (magenta) models. From top: oxygen–oxygen, oxygen–hydrogen, hydrogen–hydrogen.

by the National Science Foundation (CBET-0756641). We are grateful for the abundant computer resources provided by the Minnesota Supercomputing Institute and the Energy Smart Data Center housed in the Environmental Molecular Sciences Laboratory at PNNL. CJM is supported by the US Department of Energy's (DOE) Off ce of Basic Energy Sciences Chemical, Geosciences and Biosciences division. PNNL is operated by Battelle for the US DOE. This work performed under the auspices of the U.S. Department of Energy by Lawrence Livermore National Laboratory under Contract DE-AC52-07NA27344.

## References


[1] J. A. Barker, R. O. Watts, Chem. Phys. Lett. 3 (1969) 144–145.

[2] A. Rahman, F. H. Stillinger, J. Chem. Phys. 55 (1971) 3336–3359.

[3] W. L. Jorgensen, J. Chandrasekhar, J. D. Madura, R. W. Impey, M. L. Klein, J. Chem. Phys. 79 (1983) 926–935.

[4] H. J. C. Berendsen, J. R. Grigera, T. P. Straatsma, J. Phys. Chem. 91 (1987) 6269–6271.

[5] L. X. Dang, J. Chem. Phys. 97 (1992) 2659–2660.

[6] B. Chen, J. Xing, J. I. Siepmann, J. Phys. Chem. B 104 (2000) 2391–4201.

[7] P. Paricaud, M. Predota, A. A. Chialvo, P. T. Cummings, J. Chem. Phys 122 (2005) 244511.

[8] K. Laasonen, M. Sprik, M. Parrinello, R. Car, J. Chem. Phys. 99 (1993) 9080–9089.

[9] P. L. Silvestrelli, M. Parrinello, J. Chem. Phys. 111 (1999) 3572–3580.

[10] I.-F. W. Kuo, C. J. Mundy, M. J. McGrath, J. I. Siepmann, J. VandeVondele, M. Sprik, J. Hutter, B. Chen, M. L. Klein, F. Mohamed, M. Krack, M. Parrinello, J. Phys. Chem. B 108 (2004) 12990–12998.

[11] T. Todorova, A. P. Seitsonen, J. Hutter, I.-F. W. Kuo, C. J. Mundy, J. Phys. Chem. B 110 (2006) 3685–3691.

[12] J. L. Gao, X. F. Xia, Science 258 (1992) 631–635.

[13] M. Eichinger, P. Tavan, J. Hutter, M. Parrinello, J. Chem. Phys. 110 (1999) 10452–10467.

[14] J. L. Gao, D. G. Truhlar, Ann. Rev. Phys. Chem. 53 (2002) 467–505.

[15] R. G. Gordon, Y. S. Kim, J. Chem. Phys. 56 (1972) 3122–3133.

[16] Y. S. Kim, R. G. Gordon, J. Chem. Phys. 60 (1974) 1842–1850.

[17] D. Barker, M. Sprik, Mol. Phys. 101 (2003) 1183–1198.

[18] A. D. Becke, Phys. Rev. A 38 (1988) 3098–3100.

[19] C. Lee, W. Yang, R. G. Parr, Phys. Rev. B 37 (1988) 785–789.

[20] A. Z. Panagiotopoulos, Mol. Phys. 61 (1987) 813–826.

[21] A. Z. Panagiotopoulos, N. Quirke, M. Stapleton, D. J. Tildesley, Mol. Phys. 63 (1988) 527–545.

[22] M. J. McGrath, J. I. Siepmann, I.-F. W. Kuo, C. J. Mundy, J. VandeVondele, J. Hutter, F. Mohamed, M. Krack, J. Phys. Chem. A 110 (2006) 640–646.

[23] M. J. McGrath, J. I. Siepmann, I.-F. W. Kuo, C. J. Mundy, Mol. Phys. 104 (2006) 3619–3626.

[24] J. VandeVondele, M. Krack, F. Mohamed, M. Parrinello, T. Chassaing, J. Hutter, Comput. Phys. Comm. 167 (2005) 103–128.

[25] G. Tabacchi, J. Hutter, C. J. Mundy, J. Chem. Phys. 123 (2005) 074108.

[26] R. Iftimie, D. Salahub, D. Wei, J. Schof eld, J. Chem. Phys. 113 (2000) 4852–4862.

[27] L. D. Gelb, J. Chem. Phys. 118 (2003) 7747–7750.

[28] J. I. Siepmann, D. Frenkel, Mol. Phys. 75 (1992) 59–70.

[29] G. C. A. M. Mooij, D. Frenkel, B. Smit, J. Phys.: Condens. Matter 4 (1992) L255–L259.

[30] B. Smit, S. Karaborni, J. I. Siepmann, J. Chem. Phys. 102 (1995) 2126–2140.

[31] T. J. H. Vlugt, M. G. Martin, B. Smit, J. I. Siepmann, R. Krishna, Mol. Phys. 94 (1998) 727–733.

[32] H. Lee, C. Lee, R. G. Parr, Phys. Rev. A 44 (1991) 768–771.

[33] M. J. McGrath, J. I. Siepmann, I.-F. W. Kuo, C. J. Mundy, J. VandeVondele, J. Hutter, F. Mohamed, M. Krack, ChemPhysChem 6 (2005) 1894–1901.

[34] J. S. Rowlinson, B. Widom, Molecular Theory of Capillarity, Oxford University Press, New York, 1989.

[35] J. S. Rowlinson, F. L. Swinton, Liquids and Liquid Mixtures, Butterworth, London, 1982.

[36] P. W. Atkins, Physical Chemistry, Oxford University Press, 2002.

[37] M. J. McGrath, J. I. Siepmann, I.-F. W. Kuo, C. J. Mundy, Mol. Phys. 105 (2007) 1411–1417.

[38] J. Schmidt, J. VandeVondele, I-F. W. Kuo, D. Sebastiani, J. I. Siepmann, J. Hutter, C. J. Mundy, J. Phys. Chem. B (2009) submitted for publication.

[39] NIST Chemistry WebBook, NIST Standard Reference Database Number 69, Eds. P.J. Linstrom and W.G. Mallard, June 2005, National Institute of Standards and Technology, Gaithersburg MD, 20899 (http://webbook.nist.gov).

[40] J. R. Errington, A. Z. Panagiotopoulos, J. Phys. Chem. B 102 (1998) 7470–7475.

[41] B. Chen, J. J. Potoff, J. I. Siepmann, J. Phys. Chem. B 104 (2000) 2378–2390.

[42] G. Hura, D. Russo, R. M. Glaeser, T. Head-Gordon, M. Krack, M. Parrinello, Phys. Chem. Chem. Phys. 5 (2003) 1981–1991.